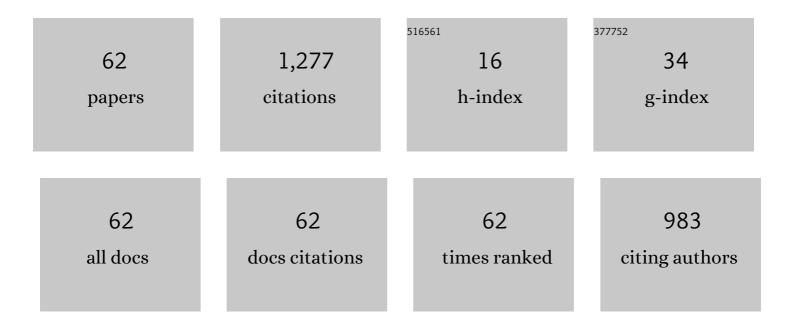
List of Publications by Year in descending order

Source: https://exaly.com/author-pdf/3187826/publications.pdf Version: 2024-02-01



ΔΝΙΟΡΕΙΙ ΒΛΟΛΙ

#	Article	IF	CITATIONS
1	Accelerating Monte Carlo simulations of photon transport in a voxelized geometry using a massively parallel graphics processing unit. Medical Physics, 2009, 36, 4878-4880.	1.6	264
2	A <scp>PENELOPE</scp> â€based system for the automated Monte Carlo simulation of clinacs and voxelized geometries—application to farâ€fromâ€axis fields. Medical Physics, 2011, 38, 5887-5895.	1.6	217
3	Evaluation of Digital Breast Tomosynthesis as Replacement of Full-Field Digital Mammography Using an In Silico Imaging Trial. JAMA Network Open, 2018, 1, e185474.	2.8	121
4	Monte Carlo reference data sets for imaging research: Executive summary of the report of AAPM Research Committee Task Group 195. Medical Physics, 2015, 42, 5679-5691.	1.6	76
5	A novel physical anthropomorphic breast phantom for 2D and 3D xâ€ray imaging. Medical Physics, 2017, 44, 407-416.	1.6	62
6	A package of Linux scripts for the parallelization of Monte Carlo simulations. Computer Physics Communications, 2006, 175, 440-450.	3.0	60
7	<i>penMesh</i> —Monte Carlo Radiation Transport Simulation in a Triangle Mesh Geometry. IEEE Transactions on Medical Imaging, 2009, 28, 1894-1901.	5.4	40
8	Monte Carlo modelling of Germanium detectors for the measurement of low energy photons in internal dosimetry: Results of an international comparison. Radiation Measurements, 2008, 43, 510-515.	0.7	28
9	Monte Carlo simulation of MOSFET detectors for high-energy photon beams using the PENELOPE code. Physics in Medicine and Biology, 2007, 52, 303-316.	1.6	25
10	Evaluation of data augmentation via synthetic images for improved breast mass detection on mammograms using deep learning. Journal of Medical Imaging, 2019, 7, 1.	0.8	25
11	Technical Note: In silico imaging tools from the VICTRE clinical trial. Medical Physics, 2019, 46, 3924-3928.	1.6	24
12	X-ray properties of an anthropomorphic breast phantom for MRI and x-ray imaging. Physics in Medicine and Biology, 2011, 56, 3513-3533.	1.6	23
13	Mammography and breast tomosynthesis simulator for virtual clinical trials. Computer Physics Communications, 2021, 261, 107779.	3.0	23
14	Stable gelatin-based phantom materials with tunable x-ray attenuation properties and 3D printability for x-ray imaging. Physics in Medicine and Biology, 2018, 63, 09NT01.	1.6	21
15	Monte Carlo simulation of X-ray imaging using a graphics processing unit. , 2009, , .		20
16	Spatiotemporal Monte Carlo transport methods in x-ray semiconductor detectors: Application to pulse-height spectroscopy in a-Se. Medical Physics, 2011, 39, 308-319.	1.6	19
17	Monte Carlo simulation of novel breast imaging modalities based on coherent x-ray scattering. Physics in Medicine and Biology, 2014, 59, 3501-3516.	1.6	16
18	Reproducing two-dimensional mammograms with three-dimensional printed phantoms. Journal of Medical Imaging, 2018, 5, 1.	0.8	16

#	Article	IF	CITATIONS
19	hybrid\$scriptsize{mathrm{MANTIS}}\$: a CPU–GPU Monte Carlo method for modeling indirect x-ray detectors with columnar scintillators. Physics in Medicine and Biology, 2012, 57, 2357-2372.	1.6	15
20	Monte Carlo simulation of a realistic anatomical phantom described by triangle meshes: Application to prostate brachytherapy imaging. Radiotherapy and Oncology, 2008, 86, 99-103.	0.3	14
21	Maximum-likelihood estimation of scatter components algorithm for x-ray coherent scatter computed tomography of the breast. Physics in Medicine and Biology, 2016, 61, 3164-3179.	1.6	10
22	Fast Monte Carlo codes for occupational dosimetry in interventional radiology. Physica Medica, 2021, 85, 166-174.	0.4	10
23	Monte Carlo package for simulating radiographic images of realistic anthropomorphic phantoms described by triangle meshes. , 2007, , .		9
24	Monte Carlo simulation of amorphous selenium imaging detectors. , 2010, , .		9
25	A real-time radiation dose monitoring system for patients and staff during interventional fluoroscopy using a GPU-accelerated Monte Carlo simulator and an automatic 3D localization system based on a depth camera. Proceedings of SPIE, 2013, , .	0.8	9
26	Monte Carlo X-ray transport simulation of small-angle X-ray scattering instruments using measured sample cross sections. Journal of Applied Crystallography, 2016, 49, 188-194.	1.9	9
27	Reproducing 2D breast mammography images with 3D printed phantoms. Proceedings of SPIE, 2016, , .	0.8	9
28	In silico imaging clinical trials for regulatory evaluation: initial considerations for VICTRE, a demonstration study. Proceedings of SPIE, 2017, , .	0.8	9
29	A database for estimating organ dose for coronary angiography and brain perfusion CT scans for arbitrary spectra and angular tube current modulation. Medical Physics, 2012, 39, 5336-5346.	1.6	8
30	Feasibility of estimating volumetric breast density from mammographic xâ€ray spectra using a cadmium telluride photonâ€counting detector. Medical Physics, 2018, 45, 3604-3613.	1.6	8
31	Computational reader design and statistical performance evaluation of an in-silico imaging clinical trial comparing digital breast tomosynthesis with full-field digital mammography. Journal of Medical Imaging, 2020, 7, 1.	0.8	8
32	Reducing radiation dose to the female breast during CT coronary angiography: A simulation study comparing breast shielding, angular tube current modulation, reduced kV, and partial angle protocols using an unknown-location signal-detectability metric. Medical Physics, 2013, 40, 081921.	1.6	7
33	Fast cardiac CT simulation using a graphics processing unit-accelerated Monte Carlo code. , 2010, , .		6
34	Reducing the Memory Requirements of High Resolution Voxel Phantoms by Means of a Binary Tree Data Structure. IEEE Transactions on Radiation and Plasma Medical Sciences, 2019, 3, 76-82.	2.7	6
35	Reducing overfitting of a deep learning breast mass detection algorithm in mammography using synthetic images. , 2019, , .		6
36	Monte Carlo simulated coronary angiograms of realistic anatomy and pathology models. , 2007, , .		5

#	Article	IF	CITATIONS
37	Use of an electron spoiler for radiation treatment of surface skin diseases. Clinical and Translational Oncology, 2010, 12, 374-380.	1.2	5
38	Virtual clinical trial for task-based evaluation of a deep learning synthetic mammography algorithm. , 2019, , .		5
39	A physical breast phantom for 2D and 3D x-ray imaging made through inkjet printing. Proceedings of SPIE, 2017, , .	0.8	4
40	Fast Simulation of Radiographic Images Using a Monte Carlo X-Ray Transport Algorithm Implemented in CUDA. , 2011, , 813-829.		3
41	A Task-Specific Argument for Variable-Exposure Breast Tomosynthesis. Lecture Notes in Computer Science, 2012, , 72-79.	1.0	3
42	An efficient depth- and energy-dependent Monte Carlo model for columnar CsI detectors. , 2008, , .		2
43	A GPU-optimized binary space partition structure to accelerate the Monte Carlo simulation of CT projections of voxelized patient models with metal implants. , 2012, , .		2
44	Dosimetric impact of voxel resolutions of computational human phantoms for external photon exposure. Biomedical Physics and Engineering Express, 2019, 5, 065002.	0.6	2
45	Exploring CNN potential in discriminating benign and malignant calcifications in conventional and dual-energy FFDM: simulations and experimental observations. Journal of Medical Imaging, 2021, 8, 033501.	0.8	2
46	Monte Carlo Simulation of a-Se X-ray Detectors for Breast Imaging: Effect of Nearest-Neighbor Recombination Algorithm on Swank Noise. Lecture Notes in Computer Science, 2012, , 575-582.	1.0	2
47	A Review of Doses for Dental Imaging in 2010–2020 and Development of a Web Dose Calculator. Radiology Research and Practice, 2021, 2021, 1-18.	0.6	2
48	Designing a phantom for dose evaluation in multi-slice CT. , 2010, , .		1
49	Energy deposition in the breast during CT scanning: quantification and implications for dose reduction. , 2011, , .		1
50	A mathematical framework for including various sources of variability in a task-based assessment of digital breast tomosynthesis. Proceedings of SPIE, 2012, , .	0.8	1
51	Method to study sample object size limit of small-angle x-ray scattering computed tomography. Proceedings of SPIE, 2016, , .	0.8	1
52	Using convolutional neural networks to discriminate between cysts and masses in Monte Carloâ€simulated dualâ€energy mammography. Medical Physics, 2021, 48, 4648-4655.	1.6	1
53	Method to measure the size of a radiographic field larger than a detector by imaging fluorescence Xâ€rays with a slit camera. Journal of Applied Clinical Medical Physics, 2021, 22, 222-231.	0.8	1
54	Classification of breast calcifications in dual-energy FFDM using a convolutional neural network: simulation study. , 2020, , .		1

#	Article	IF	CITATIONS
55	Analyzing neural networks applied to an anatomical simulation of the breast. , 2022, , .		1
56	Spatio-temporal Monte Carlo modeling of a-Se detectors for breast imaging: energy-weighted Swank noise and detective quantum efficiency. Proceedings of SPIE, 2012, , .	0.8	0
57	Spatial resolution characteristics of a-Se imaging detectors using Monte Carlo methods with detailed spatiotemporal transport of x-rays, electrons, and electron-hole pairs under applied bias. , 2013, , .		0
58	Prototype adaptive bow-tie filter based on spatial exposure time modulation. , 2016, , .		0
59	Classification of round lesions in dual-energy FFDM using a convolutional neural network: simulation study. , 2021, , .		О
60	WE-G-110-06: Introduction to the AAPM Task Group No. 195 - Monte Carlo Reference Data Sets for Imaging Research. Medical Physics, 2011, 38, 3834-3834.	1.6	0
61	Monte Carlo Modeling of the DQE of a-Se X-Ray Detectors for Breast Imaging. Lecture Notes in Computer Science, 2014, , 387-393.	1.0	Ο
62	Mammographic Image Conversion Between Source and Target Acquisition Systems Using cGAN. Lecture Notes in Computer Science, 2020, , 523-531.	1.0	0